International Journal of Thermophysics, Vol. 23, No. 1, January 2002 (© 2002)

# Measurements of the Thermal Conductivities of Solid and Liquid Unbranched Alkanes in the $C_{16}$-to-$C_{19}$ Range During Phase Transition[1]

**R. Holmen,[2,3] M. Lamvik,[4] and O. Melhus[4]**

This paper presents thermal conductivities for both solid and liquid unbranched alkanes ranging from $C_{16}$ to $C_{19}$. The thermal conductivities are measured with a method which gives both liquid and solid thermal conductivities at the temperature of phase transition. An assessment of the error of the method has been performed. The measurements of solid conductivities are in accordance with measurements reported previously and confirm the applicability of the method. Experimental liquid conductivities are higher than extrapolated values from the literature, but this is believed to be caused by structural changes which occur close to the melting-point temperature.

**KEY WORDS:** heat conduction; heptadecane; hexadecane; nonadecane; octadecane; phase transition; thermal conductivity.

## 1. INTRODUCTION

During transportation and production of crude oils, heavy components, i.e., wax, tend to deposit on the walls of pipelines and process equipment. This deposition of wax may lead to reduced capacity and eventually to plugging of pipelines. This problem is particularly serious during transportation of crude oils in a cold environment, as in the North Sea. The deposited wax is a mixture of different hydrocarbons, but a substantial part [1] consists of *n*-paraffinic waxes.

[1] Paper presented at the Fourteenth Symposium on Thermophysical Properties, June 25–30, 2000, Boulder, Colorado, U.S.A.

[2] Nammo Raufoss AS, Postboks 162, N-2831 Raufoss, Norway.

[3] To whom correspondence should be addressed. E-mail: rune.holmen@raufoss.nammo.com

[4] Department of Applied Mechanics, Thermodynamics and Fluid Dynamics, The Norwegian University of Science and Technology, NTNU, N-7491 Trondheim, Norway.



0195-928X/02/0100-0027/0 © 2002 Plenum Publishing Corporation

Much work has been done to model the solid–liquid equilibria of petroleum waxes. A review of such models is given by Pauly et al. [2] or by Coutinho et al. [3].

Simulations of wax precipitation are helpful both prior to construction and during operation of pipelines. The quality of these simulations depends on the quality of the input data. The physical properties around the melting point are of particular interest. Since predicting wax formation is a question of solving the temperature field, it is surprising to note the low attention given to the determination of the thermal conductivities around the melting-point temperature.

Liquid conductivities are reported by Vargaftik [4]. Griggs and Yarbrough [5] report measurements of the thermal conductivity of solid, unbranched $C_{16}$, $C_{17}$, $C_{18}$, and $C_{19}$, while Yarbrough and Kuan [6] have measured the conductivities of $C_{17}$ and $C_{18}$. Forsman and Andersson [7] have measured thermal conductivities at high pressures of solid odd-numbered *n*-alkanes ranging from $C_9H_{20}$ to $C_{19}H_{40}$. Irby et al. [8] have resolved disagreement in the reported values of the thermal conductivity of solid octadecane by conducting additional measurements with various techniques.

This paper presents data for the thermal conductivity for both the solid and the liquid phases at the temperature of phase transition. The number of C atoms of the investigated *n*-paraffinic waxes ranges from 16 to 19. The method employed is a minor modification of the method developed by Lamvik and Zhou [9].

## 2. THEORY

Considering the situation as shown in Fig. 1, Lamvik and Zhou [9] gave Neumann's general condition at the phase interface as

$$-k_s \frac{\partial T_s}{\partial x} + k_l \frac{\partial T_l}{\partial x} + \rho h_{mp} \frac{dx_{mp}}{dt} = 0 \tag{1}$$

where $\rho$ is the density of the disappearing phase, $k_s$ and $k_l$ are, respectively, the solid and liquid thermal conductivities, and $h_{mp}$ is the enthalpy of phase transition. Assuming that the temperature at the bottom, $T_0$, is lower than at the top, $T_H$, the temperature gradients in the solid, $\partial T_s/\partial x$, and in the liquid, $\partial T_l/\partial x$, are both positive. During freezing, the position of the interface, $x_{mp}$, is moving upward, i.e., the speed of the interface, $dx_{mp}/dt$, is positive. Equation (1) is simplified by choosing proper experimental conditions, i.e., melting or freezing with the temperature gradient only in the appearing phase.

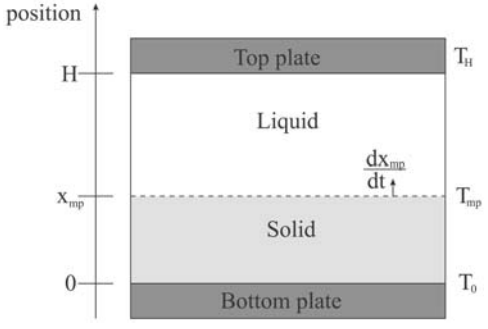


**Fig. 1.** Schematic of phase transition.

No thermal gradient in the liquid phase gives

$$k_s = \rho_l h_{mp} \frac{dx_{mp}}{dt} \left( \frac{\partial T_s}{\partial x} \right)^{-1} \tag{2}$$

Assuming melting, and no thermal gradient in the solid phase, one finds

$$k_l = -\rho_s h_{mp} \frac{dx_{mp}}{dt} \left( \frac{\partial T_l}{\partial x} \right)^{-1} \tag{3}$$

Introducing thermal equilibrium in Eq. (1), the ratio of the conductivities appears as

$$\frac{k_l}{k_s} = \frac{\partial T_s / \partial x}{\partial T_l / \partial x} \tag{4}$$

Equations (2), (3), and (4) are the working equations of this study.

To be able to use the results from experiments to calculate thermal conductivities from the working equations, approximations to the derivatives must be found. Denoting the total height of the cell as $H$ and assuming that the thermal gradients are linear, estimates of $\partial T / \partial x$ are

$$\frac{\partial T_l}{\partial x} \approx \frac{T_H - T_{mp}}{H - x_{mp}} \tag{5}$$

and

$$\frac{\partial T_s}{\partial x} \approx \frac{T_{mp} - T_0}{x_{mp}} \tag{6}$$

Suppose that the position of the interface is measured at heights at a predetermined interval denoted $\Delta x$, $dx_{mp}(t)/dt$ can be approximated as

$$\frac{dx_{mp}(t)}{dt} \approx \frac{2\Delta x}{t(x_{mp}+\Delta x)-t(x_{mp}-\Delta x)} \tag{7}$$

## 3. EXPERIMENTAL

The experimental procedure is a modification of the method presented by Lamvik and Zhou [9].

### 3.1. Apparatus

The apparatus was the same as used by Lamvik and Zhou [9]. The only exception was the thermostated liquid reservoirs. Figure 2 is a schematic of the equipment used in this investigation. The experimental cell consists of two circular plates with a cylindrical glass ring between. A cylindrical cavity with a diameter of 60 mm was formed between the plates.

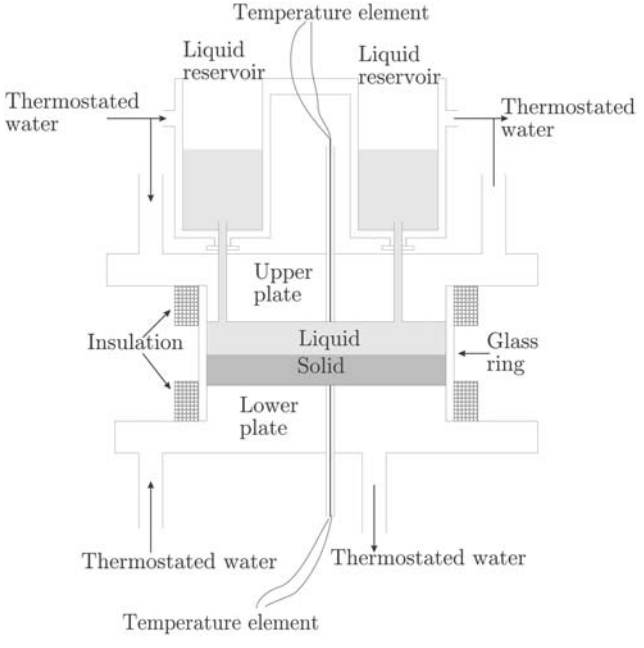


**Fig. 2.** Experimental cell.

The height of the cavity, $H$, was 12 to 12.8 mm. The plates were channeled and connected via a system of valves to two thermostated water baths. The system of valves made it possible to connect the plates either to the same bath or to the separate baths.

A ring of expanded polyester was used as insulation outside the glass ring. A hole in the insulation made it possible to use a cathetometer to measure the level of the interface. The liquid reservoirs were also channeled, and thermostated water was pumped through them. The temperatures of the reservoirs were always maintained as close as possible to the temperature of the upper plate.

Measurements of temperature were carried out by inserting temperature elements into pockets in the plates. The elements were of Type K. The reference junctions were kept at 0°C and the voltage was read from a Fluke 45 voltmeter. The voltage was correlated with temperature using data from Powell et al. [10]. Time was measured by reading the time from a Casio Travel & Clock TC-1000. A cathetometer, Model LS 701 from Heidehain, was used to measure the position of the interface.

### 3.2. Chemicals

All chemicals were delivered from Merck. According to Merck, hexadecane ($C_{16}$), heptadecane ($C_{17}$), and octadecane ($C_{18}$) were more than 99% pure, while the purity of nonadecane ($C_{19}$) exceeded 98%. No information was provided regarding the nature of the impurities.

### 3.3. Procedures

Prior to all experiments, the cell was washed with appropriate wax and then filled with liquid wax through the liquid reservoirs. To ensure that a minimum amount of gas was dissolved in the wax, the wax was repeatedly frozen and thawed until no bubbles appeared. The bubbles were removed by tilting the cell so that the they could escape through the liquid reservoirs. Both the cell and the cathetometer were leveled using a carpenter's level. To assure that the liquid in the cell could communicate with the liquid in the reservoirs, all freezing was done from the bottom and up.

To find the setpoints of the water baths closest to the melting point, the wax was frozen and the temperature of the upper plate was gradually increased in steps of 0.1 K until melting started. Before commencing with measurements, the wax in the cell was melted by increasing the temperature of the plates above the melting point.

### *3.3.1. Solid Thermal Conductivity*

The temperatures of the plates were reduced to the melting-point temperature. After more than 1 h of thermal equilibration, the temperature of the lower plate was reduced to the desired temperature. The cathetometer was raised at least 0.5 mm above the lower plate. When the interface reached the cathetometer, the time was recorded. The cathetometer was then raised in intervals, normally 0.2 mm. The time and position of the interface were recorded at each interval. Measurements were made at at least five levels. The temperatures of the plates were continuously monitored and recorded.

### *3.3.2. Liquid Thermal Conductivity*

The wax in the cell was frozen by reducing the temperature of the lower plate below the melting-point temperature, while the temperature of the upper plate was kept at the melting-point temperature. When the wax was solid, the temperature of the lower plate was increased to the melting point. After more than 1 h of thermal equilibration, the temperature of the upper plate was increased to the desired temperature. The cathetometer was positioned at least 0.5 mm under the top plate. When the interface reached the cathetometer, time was recorded. The cathetometer was then lowered in intervals, normally 0.2 mm. The time and position of the interface were recorded at each interval. Measurements were made at at least five levels. The temperatures of the plates were continuously monitored and recorded.

### *3.3.3. Ratio of Solid and Liquid Conductivities*

The wax in the cell was frozen by reducing the temperature of the lower plate to the desired temperature while the temperature of the upper plate was kept at the melting-point temperature. The temperature of the upper plate was then raised to the desired level, and after equilibration overnight, the position of the interface and temperatures of the plates were recorded.

## 4. RESULTS

Experiments were performed as described above. Calculations of the thermal conductivities were done by utilizing Eqs. (2)–(4). Between five and seven experiments were performed for each component. For each experiment conducted to find the liquid or solid conductivity, at least three values were calculated. The averaged results are given in Table I.

**Table I.** Results from Experiments

| | Hexadecane | Heptadecane | Octadecane | Nonadecane |
|---|---|---|---|---|
| $k_l$ ($W \cdot m^{-1} \cdot K^{-1}$) | 0.21 | 0.22 | 0.18 | 0.23 |
| $k_s$ ($W \cdot m^{-1} \cdot K^{-1}$) | 0.29[a] | 0.19[a] | 0.31[a] | 0.14[a] |
| $k_l/k_s$ | 0.53 | 1.0 | 0.45 | 1.0 |

[a] These measurements were disregarded. $k_s$ was calculated from measurements of $k_l$ and $k_l/k_s$. See Section 5.2.2.

## 5. DISCUSSION

### 5.1. Random Errors

#### *5.1.1. Measurement of Temperature*

The measurements of temperature were made by using thermocouples as described earlier. The error in the temperature measurements was estimated to be $\sigma_T = 0.25$ K.

#### *5.1.2. Measurement of the Position of the Interface*

Measurements of the position of the interface were done as described by using a cathetometer. When measuring the position of a clear and steady object, it was possible to determine the position within 0.01 mm. The border between the solid and the liquid phases was not clear or steady, so this position could not be measured closer than to the nearest 0.05 mm, i.e., $\sigma_x = 0.025$ mm $= 0.025 \times 10^{-3}$ m.

#### *5.1.3. Measurement of Time*

Time was read off an ordinary digital watch from Casio. There is no reason to anticipate a more noticeable error than that due to moving the eye from the measurement of position to the clock, i.e., $\sigma_t = 1$ s.

### 5.2. Systematic Errors

#### *5.2.1. Errors in Physical Constants*

The reported melting points in the literature differed by up to 0.3 K. The maximum discrepancy was found for $T_{mp}^{C16}$. Finke et al. [11] report that $T_{mp}^{C16} = 291.34$ K, while Parks et al. [12] report that $T_{mp}^{C16} = 291.1$ K. Impurities in the chemicals used might have been responsible for additional uncertainty. Assuming that the reported melting points found in Refs. 12–14 are reliable to the closest 0.5 K, $\sigma_{T_{mp}}$ can be estimated to 0.25 K.

The densities of the solid phase of $C_{16}$, $C_{17}$, and $C_{18}$ were calculated from the liquid density. The shrinkage was assumed to be 10%, which is equivalent to the shrinkage at solidification reported by Schaerer et al. [13] for other *n*-paraffinic waxes. This assumption is uncertain, and thus, $\sigma_\rho = 100\ \mathrm{kg \cdot m^{-3}}$.

The enthalpies of melting in the literature [11–14] differed so much that $h_{mp}$ could not be determined more precisely than to the closest 10,000 $\mathrm{J \cdot kg^{-1}}$, i.e., $\sigma_{h_{mp}} = 5000\ \mathrm{J \cdot kg^{-1}}$.

### *5.2.2. Dendritic Growth of the Solid Phase*

During measurements of the thermal conductivity of the solid phase, i.e., freezing, the solid phase grew in a dendritic manner, making measurements of the location of the interface difficult. A strong lamp was placed in the back of the experimental cell, and the position was read off at the point where no light came through. Since some precipitation did not contribute to this position, the measured speed of the interface was too low, and consequently, the calculated solid thermal conductivity was too low as well.

This is supported by the measurements of the ratio $k_l/k_s$ and the measurements of $k_l$ (see Table I). The direct measurements of the thermal conductivity of the solid phase are therefore disregarded, and $k_s$ is instead calculated from measurements of the ratio $k_l/k_s$ and the measurements of $k_l$.

### *5.2.3. Solid–Solid Equilibria*

Schaerer et al. [13] and Messerly et al. [14] reported that $C_{17}$ and $C_{19}$, but not $C_{16}$ and $C_{18}$, change solid phase at a transition point below the melting temperature. All experiments were performed above these transition points.

## 5.3. Total Assessment of Errors

### *5.3.1. Gauss's Equation for Propagation of Random Error*

An assessment of the total error in the calculation of the liquid thermal conductivities was done using Gauss's equation for propagation of random error as described by Nesse [15],

$$\sigma_{k_l} = \sqrt{\left(\sigma_{\rho_s}\frac{\partial k_l}{\partial \rho_s}\right)^2 + \left(\sigma_{h_{mp}}\frac{\partial k_l}{\partial h_{mp}}\right)^2 + \left(\sigma_{\frac{dx_{mp}}{dt}}\frac{\partial k_l}{\partial \frac{dx_{mp}}{dt}}\right)^2 + \left(\sigma_{\frac{\partial T_l(x_{mp})}{\partial x}}\frac{\partial k_l}{\partial \frac{\partial T_l(x_{mp})}{\partial x}}\right)^2} \quad (8)$$

The total error is found to be less than 17% in this experiment.

An estimate for the error in the ratio $k_l/k_s$ is done analogously

$$\sigma_{\frac{k_l}{k_s}} = \sqrt{\left(\sigma_{\frac{\partial T_l}{\partial x}} \frac{\partial(k_l/k_s)}{\partial T_l/\partial x}\right)^2 + \left(\sigma_{\frac{\partial T_s}{\partial x}} \frac{\partial(k_l/k_s)}{\partial T_s/\partial x}\right)^2} \tag{9}$$

This error is calculated to 7.1% for a typical experiment.

Finally, the error in $k_s$ is calculated as

$$\sigma_{k_s} = \sqrt{\left(\sigma_{k_l} \frac{\partial k_s}{\partial k_l}\right)^2 + \left(\sigma_{\frac{k_l}{k_s}} \frac{\partial k_s}{\partial(k_l/k_s)}\right)^2} \tag{10}$$

$\sigma_{k_s} = 18.7\%$ for $k_s$ in the calculated example.

*5.3.2. Reproducibility*

The standard deviation is used as a measure of the reproducibility. It is calculated on the basis of the seven experiments carried out to find $k_l^{C_{18}}$. The estimate of the standard deviation is found to be $\sigma_{k_l^{C_{18}}} = 0.03$ $W \cdot m^{-1} \cdot K^{-1}$, which is 17% of $k_l^{C_{18}}$, and accordingly in agreement with the estimate of accuracy based on Gauss's equation for propagation of random error.

*5.3.3. Total Assessment of Uncertainty*

Assuming that the calculation of the standard deviation and the estimate of the error found from using Gauss's equation for propagation of error are typical, an uncertainty of 20% in both $k_l$ and $k_s$ should be a conservative estimate.

## 5.4. Theoretical Assumptions

*5.4.1. Linear Temperature Gradients*

The approximations of $\partial T/\partial x$, Eqs. (5) and (6), assume linear thermal gradients. According to Grigull and Sandner [16], the Stefan number is a measure of the error associated with this assumption. For the liquid phase, the Stefan number is

$$Ph_l = \frac{h_{mp}}{Cp_l(T_l - T_{mp})} \tag{11}$$

The expression for the solid phase is

$$Ph_s = \frac{h_{mp}}{Cp_s(T_{mp} - T_s)} \tag{12}$$

Grigull and Sandner [16] show that with $Ph \geqslant 10$, the error in the approximative solution of Eq. (1) is less than 2%. $Ph \geqslant 10$ for all experiments reported in this paper. The error is consequently disregarded.

*5.4.2. Convection*

Since the measured values for the thermal conductivity of the liquids are higher than previously published, one could suspect that convection has made the heat transfer better than intended. But all experiments were conducted with the coldest part of the cell at the bottom and, thus, without a driving force for convection.

*5.4.3. No Gradient in the Unchanged Phase*

The crucial step in the derivation of the equations for calculation of the thermal conductivities, Eqs. (2) and (3), is the assumption that there is no thermal gradient in the disappearing phase. This is virtually impossible to achieve. That means that Eqs. (2) and (3) have to include an extra term, which in the liquid case is

$$k_l = \left( k_s \frac{\partial T_s(x = x_{mp})}{\partial x} - \rho_s h_{mp} \frac{dx_{mp}}{dt} \right) \left( \frac{\partial T_l(x = x_{mp})}{\partial x} \right)^{-1} \tag{13}$$

The setpoints of the water baths closest to the melting points were found by gradually increasing the temperature of solid wax in steps of 0.1 K until melting started. There is therefore no reason to anticipate an error exceeding 0.5 K.

Numerically this has the greatest impact when the gradient in the growing phase is low. Calculation for such case shows that the error is less than 2.5%. This error will always give too high a liquid thermal conductivity, but compared with the random errors, this error is negligible and is disregarded.

## 5.5. Comparisons with Previously Published Data

*5.5.1. Thermal Conductivity of Liquid* n*-Paraffinic Waxes*

Vargaftik [4] gives thermal conductivities over a large temperature range. For the components in question here, values are given for temperatures from about 590 to 313 K. These values lie on a line and seem to stem from a linear interpolation. No uncertainties are reported.

If one extrapolates Vargaftik's [4] values to the melting point, liquid conductivities for all components considered are found to be 0.15 $\mathrm{W \cdot K^{-1} \cdot m^{-1}}$. A linear interpolation of the measurements by Wada et al.

[17] of the thermal conductivity of liquid $C_{16}$ confirms the value of 0.15 $W \cdot m^{-1} \cdot K^{-1}$. This is lower than the liquid conductivities presented in this paper.

In absolute value, the measurements of Ziebland and Patient [18] are in the same range as the extrapolation of Vargaftik's [4] data, but nonlinear augmentation of thermal conductivities close to solidification is observed. They ascribe the increased conductivity with decreasing temperature to fractional crystallization.

A similar hypothesis is introduced by Earnshaw and Hughes [19]. They measured the surface tension of purified *n*-alkanes in the $C_{15}$–$C_{18}$ range. At a temperature close to, but distinct from, the melting point, they observed that the surface tension departs from the accepted steady increase to a monotonic decrease as the temperature is lowered. They assign this phenomenon to a marked reduction in the available degrees of freedom.

It is reasonable to believe that this reduction in the available degrees of freedom, i.e., entropy, becomes more significant the closer the temperature is to the melting point. A reduction in the entropy is normally connected to an increase in the thermal conductivity. It is therefore quite possible that the discrepancy between this work and the measurements in the literature [4, 17, 18] may be due to this phenomenon.

### 5.5.2. *Thermal Conductivity of Solid* n-*Paraffinic Waxes*

Griggs and Yarbrough [5] report measurements of the thermal conductivity of solid $C_{16}$, $C_{17}$, $C_{18}$, and $C_{19}$, while Yarbrough and Kuan [6] report $k_s^{C17}$ and $k_s^{C18}$. All measurements are made over a temperature range, but the variation with temperature is within their reported error and can therefore be neglected. Both papers disregard solid–solid equilibria even if the experiments are preformed well below the transition temperatures for $C_{17}$ and $C_{19}$ [13].

Irby et al. [8] have found that the reported measurements of the thermal conductivity of solid octadecane ranged from 0.15 to 0.56 $W \cdot m^{-1} \cdot K^{-1}$. They resolved this disagreement by making measurements with various techniques.

**Table II.** Comparisons of $k_s$ in ($W \cdot m^{-1} \cdot K^{-1}$) with Literature Values

| Reference | $C_{16}$ | $C_{17}$ | $C_{18}$ | $C_{19}$ |
|---|---|---|---|---|
| Griggs and Yarbrough [5] | $0.35 \pm 0.07$ | $0.21 \pm 0.06$ | $0.3 \pm 0.1$ | $0.27 \pm 0.05$ |
| Yarbrough and Kuan [6] | — | $0.19 \pm 0.02$ | $0.32 \pm 0.03$ | — |
| Forsman and Andersson [7] | — | 0.2 | — | 0.2 |
| Irby et al. [8] | — | — | $0.43 \pm 0.03$ | — |
| This work | $0.40 \pm 0.08$ | $0.22 \pm 0.04$ | $0.40 \pm 0.08$ | $0.23 \pm 0.05$ |

**Table III.** Thermal Conductivity of Solid and Liquid $C_{16}$ to $C_{19}$ at Their Melting Points

| | Hexadecane | Heptadecane | Octadecane | Nonadecane |
|---|---|---|---|---|
| $k_l$ ($W \cdot m^{-1} \cdot K^{-1}$) | $0.21 \pm 0.04$ | $0.22 \pm 0.04$ | $0.18 \pm 0.04$ | $0.23 \pm 0.05$ |
| $k_s$ ($W \cdot m^{-1} \cdot K^{-1}$) | $0.40 \pm 0.08$ | $0.22 \pm 0.04$ | $0.40 \pm 0.08$ | $0.23 \pm 0.05$ |

Their recommended value is 0.43 $W \cdot m^{-1} \cdot K^{-1}$. They explain the lower value of Griggs and Yarbrough [5] by voids.

Forsman and Andersson [7] have measured thermal conductivities at high pressures of solid odd-numbered *n*-alkanes ranging from $C_9$ to $C_{19}$. Their measurements show that the thermal conductivities are 0.2 $W \cdot m^{-1} \cdot K^{-1}$ for all investigated components at temperatures right below the melting point. They assign the low value to obstruction by orientational disorder in the rotator phase.

Results from these papers are presented together with the measurements of the solid conductivities from this study in Table II.

## 6. CONCLUSION

Thermal conductivities have been determined at the melting point for solid and liquid unbranched alkanes ranging from $C_{16}$ to $C_{19}$ . An assessment of the error of the method has been performed. The measurements of solid conductivities are in accordance with measurements reported previously and confirm the applicability of the method. Experimental liquid conductivities are higher than extrapolated values from the literature, but this is believed to be caused by structural changes which occur close to the melting-point temperature. The results are presented in Table III.

## ACKNOWLEDGMENT

The realization of this work was rendered feasible by financial aid from STATOIL and the Norwegian Research Council.

## REFERENCES

1. H. Rønningsen, B. Bjørdal, A. Hansen, and W. Pedersen, *Energy Fuels* **5** (1991).
2. J. Pauly, C. Dauphin, and J. L. Daridon, *Fluid Phase Equil.* **149**:191 (1998).
3. J. Coutinho, S. I. Andersen, and E. H. Stenby, *Fluid Phase Equil.* **103**:23 (1995).
4. N. B. Vargafitk, *Tables on the Thermophysical Properties of Liquids and Gases*, 2nd ed. (John Wiley, Washington, DC–London, 1975).
5. E. I. Griggs and D. W. Yarbrough, *Proc. Southeast. Semin. Therm. Sci.* (North Carolina state University, Raleigh, 1978).

6. D. W. Yarbrough and C.-N. Kuan, *Proc. 17th Int. Therm. Conduct. Conf.* (Plenum Press, New York, 1983).
7. H. Forsman and P. Andersson, *J. Chem. Phys.* **80**:2804 (1984).
8. R. G. Irby, J. R. Parsons, and E. G. Keshok, *Therm. Conduct.* **19**:121 (1988).
9. M. Lamvik and J. M. Zhou, *Int. J. Thermophys.* **16**:567 (1995).
10. R. L. Powell, W. J. Hall, J. C . H. Hyink, L. L. Sparks, G. W. Burns, M. G. Scroger, and H. H. Plumb, *Thermocouple Reference Tables Based on the IPTS-68* (U.S. Department of Commerce, National Bureau of Standards, Washington, DC–Boulder, 1974).
11. H. Finke, M. Gross, G. Waddington, and H. Huffman, *J. Am. Chem. Soc.* **76**:333 (1954).
12. G. Parks, G. Moore, M. Renquist, B. Naylor, L. A. McClaine, P. Fujii, and J. Hatton, *J. Am. Chem. Soc.* **71**:3386 (1949).
13. A. A. Scaerer, C. J. Busco, A. E. Smith, and L. B. Skinner, *J. Am. Chem. Soc.* **77**:2017 (1955).
14. J. F. Messerly, G. B. Guthrie, S. S. Todd, and H. L. Finke, *J. Chem. Eng. Data* **12**:338 (1967).
15. N. Nesse, *Beregning av usikkerheten ved må linger* (Institutt for Kjemiteknikk, NTH, Trondheim, 1968).
16. U. Grigull and H. Sandner, *Wärmeleitung* (Springer-Verlag, Berlin, 1979).
17. Y. Wada, Y. Nagasaka, and A. Nagashima, *Int. J. Thermophys.* **6**:251 (1985).
18. H. Ziebland and J. E. Patient, *J. Chem. Eng. Data* **7**:530 (1962).
19. J. C. Earnshaw and C. J. Hughes, *Phys. Rev. A* **46**:4494 (1992).